Received: 30 March 2022 | Revised: 6 July 2022 | Accepted: 19 July 2022

DOI: 10.1002/mgg3.2029

Molecular Genetics & Genomic Medicine Open Access WILEY

ORIGINAL ARTICLE

X-chromosomal inactivation patterns in women with Fabry disease

Laura Wagenhäuser[1] | **Vanessa Rickert**[1] | **Claudia Sommer**[1,2] | **Christoph Wanner**[2,3] | **Peter Nordbeck**[2,4] | **Simone Rost**[5] | **Nurcan Üçeyler**[1,2]

[1]Department of Neurology, University of Würzburg, Würzburg, Germany

[2]Fabry Centre for Interdisciplinary Therapy Würzburg (FAZIT), University of Würzburg, Würzburg, Germany

[3]Department of Internal Medicine, Division of Nephrology, University of Würzburg, Würzburg, Germany

[4]Department of Internal Medicine, Division of Cardiology, University of Würzburg, Würzburg, Germany

[5]Institute of Human Genetics, University of Würzburg, Würzburg, Germany

Correspondence
Nurcan Üçeyler, Department of Neurology, University of Würzburg, Josef-Schneider-Str. 11, 97080 Würzburg, Germany.
Email: ueceyler_n@ukw.de

Funding information
Deutsche Forschungsgemeinschaft, Grant/Award Number: SFB 1158 and UE171/15-1; Takeda Pharmaceuticals International AG, Grant/Award Number: IIR-DEU-000798

Abstract

Background: Although Fabry disease (FD) is an X-linked lysosomal storage disorder caused by mutations in the α-galactosidase A gene (*GLA*), women may develop severe symptoms. We investigated X-chromosomal inactivation patterns (XCI) as a potential determinant of symptom severity in FD women.

Patients and Methods: We included 95 women with mutations in *GLA* ($n = 18$ with variants of unknown pathogenicity) and 50 related men, and collected mouth epithelial cells, venous blood, and skin fibroblasts for XCI analysis using the methylation status of the androgen receptor gene. The mutated X-chromosome was identified by comparison of samples from relatives. Patients underwent genotype categorization and deep clinical phenotyping of symptom severity.

Results: 43/95 (45%) women carried mutations categorized as classic. The XCI pattern was skewed (i.e., ≥75:25% distribution) in 6/87 (7%) mouth epithelial cell samples, 31/88 (35%) blood samples, and 9/27 (33%) skin fibroblast samples. Clinical phenotype, α-galactosidase A (GAL) activity, and lyso-Gb3 levels did not show intergroup differences when stratified for X-chromosomal skewing and activity status of the mutated X-chromosome.

Conclusions: X-inactivation patterns alone do not reliably reflect the clinical phenotype of women with FD when investigated in biomaterial not directly affected by FD. However, while XCI patterns may vary between tissues, blood frequently shows skewing of XCI patterns.

KEYWORDS

Fabry disease, Fabry genotype, Fabry phenotype, female Fabry patients, X-chromosomal inactivation

1 | INTRODUCTION

Fabry disease (FD) is an X-chromosomal disorder caused by mutations in the gene encoding alpha-galactosidase A (*GLA*). Impaired enzyme function leads to FD as a lysosomal storage disorder with cellular deposition of sphingolipids, among others also of globotriaosylceramide (Gb3), and subsequent multiorgan involvement (Germain, 2010). Although FD follows X-linked inheritance, women may reach any level of disease severity

(Wilcox et al., 2008). While the reason for this phenomenon is unclear, the impact of individual X-chromosomal inactivation patterns is assumed in analogy to other X-linked diseases such as Duchenne muscular dystrophy (Mercier et al., 2013) or hemophilia A and B (Garagiola et al., 2021). In some studies, a potential link between X-inactivation patterns and clinical FD phenotype was described (Dobrovolny et al., 2005; Echevarria et al., 2016; Hossain et al., 2019); however, these findings were not confirmed by others (Elstein et al., 2012; Juchniewicz et al., 2018; Rossanti et al., 2021).

We investigated a large and clinically well-characterized cohort of women carrying *GLA* variants and analyzed the link of X-inactivation patterns with the clinical phenotype and blood parameters as a potential prognostic biomarker in clinical application.

2 | PATIENTS AND METHODS

2.1 | Recruitment

We recruited 154 study participants at our Fabry Center for Interdisciplinary Therapy (FAZIT), University Hospital of Würzburg, Germany, who were seen between August 2018 and March 2020. Our cohort consisted of 104 women with sequence variants in the *GLA* gene and 50 related men who were either healthy or FD mutation carriers. This setting allowed unequivocal determination of the mutated X-chromosome in the respective women. The Würzburg Medical Faculty Ethics Committee (#259/17) approved our study and written informed consent was obtained from all patients before inclusion.

2.2 | Classification of genetic sequence variants

Genotype was determined before the first interview at FAZIT and respective reports were provided by the patients or by Centogene (Rostock, Germany). The sequence variants were categorized by three classification systems: (1) Based on the observed clinical phenotype caused by the sequence variant, i.e., classic, late-onset, benign, and variant of unknown significance (VUS) (Arends et al., 2017). For individual classification, the Fabry database was used (http://www.dbfgp.org). (2) Based on the five pathogenicity classes of sequence variants according to the American College of Medical Genetics and Genomics (ACMG) (Richards et al., 2015), i.e., benign (equivalent to "class 1"), likely benign ("class 2"), VUS ("class 3"), VUS with probable pathogenicity ("class 3+") (Kolokotronis et al., 2020), likely pathogenic ("class 4"), and pathogenic ("class 5"). The allocation to these classes was achieved by evaluating the information from Alamut Visual version 2.11 (Interactive Biosoftware, Rouen, France) providing the data of various population and mutation databases, different prediction tools, as well as information from the literature. (3) Based on the localization of missense variants (i.e., amino acid substitutions) in the final enzyme defining the categories of mutations found in the "active site", "buried" mutations, and "other" mutations (Garman & Garboczi, 2004; Rickert et al., 2020); for this, the 3D-structure of GAL obtained from the Protein Data Bank (PDB) in Europe (https://www.rcsb.org/structure/1R46 2003) was analyzed in PyMOL 1.8 graphics system (Delano, 2015). For each missense variant, the individual localization of the amino acid exchange in the final enzyme was determined. We used these three classification systems for comprehensive stratification of our patients to draw attention to the diversity of classification systems and the heterogeneity of patient grouping depending on the systems applied.

2.3 | Clinical and laboratory phenotyping

Patients underwent a detailed medical interview, complete neurological and general medical examination, and filled in the Würzburg Fabry Pain Questionnaire (FPQ) (Magg et al., 2015). Additionally, medical reports were screened for past transient ischemic attacks (TIA) or cerebral stroke as hints of central nervous system involvement. The diagnosis of small fiber neuropathy was made in accordance with published criteria (Devigili et al., 2008). Cardiomyopathy was detected by signs of left ventricular hypertrophy in echocardiography and late gadolinium enhancement (LGE) in magnetic resonance imaging (MRI). Nephropathy was diagnosed by evaluation of the glomerular filtration rate and the albumin:creatinine ratio in morning spot urine. For better comparability of our subgroups, we calculated a numeric score that describes the clinical phenotype by symptom severity. We assigned one point for each involved organ system including kidneys, heart, central nervous system, and pain, resulting in: 0 points = no, 1 point = mild, 2 points = moderate, ≥3 points = severe clinical symptoms.

GAL enzyme activity was measured in leucocytes (Podskarbi Laboratory, Munich, Germany; normal range: 0.4–1.0 nmol/min/mg). Plasma lyso-Gb3 was assessed by Centogene (Rostock, Germany) using liquid chromatography and mass spectrometry (normal range: <0.9 ng/ml).

2.4 | Biomaterial collection

We investigated mouth epithelial cells, venous blood, and skin fibroblasts. Mouth epithelial cells were collected

using swabs (Copan Diagnostics Inc., Brescia, Italy). 2.7 ml of venous blood was drawn in a tube containing ethylene-diamine-tetra-acetate (EDTA). Skin fibroblasts were obtained from diagnostic 6-mm skin punch biopsies taken from the lower leg and cultured as described earlier (Karl et al., 2019; Üçeyler et al., 2010). In men, the mutated X-chromosome was determined only in mouth epithelial cells. Follow-up samples for the investigation of biological replicates (mouth epithelial cells, blood) were collected within a median of 1 year (range 0.2–3.0 years) from a subgroup of 49/95 (52%) women.

2.5 | DNA extraction

DNA was extracted with the QIAmp DNA mini kit (Quiagen, Venlo, Netherlands) following the manufacturer's instructions with slight modifications. All DNA samples were stored at −20°C until X-inactivation analysis.

2.6 | X-inactivation analysis

X-chromosomal inactivation (XCI) analysis was performed by enzymatic methylation assessment of the human androgen receptor gene (*AR*, MIM 313700) located on Xq12 using methods and primers as described earlier (Allen et al., 1992) with minor modifications. After determining DNA concentrations with the Qubit fluorometer (Invitrogen AG, Carlsbad, California, USA), DNA dilution of 10 ng/µl in TE buffer (containing TRIS and EDTA) was prepared. Additionally, the methylation-sensitive restriction enzyme *HhaI* and the appropriate reaction buffer were added to the DNA dilution and incubated following the manufacturer's instructions (Promega, Madison, Wisconsin, USA). Patient DNA was treated accordingly, however, no *HhaI* enzyme was added allowing comparison of digested (= non-methylated) versus non-digested (= methylated) DNA and exact calculation of X-chromosomal methylation degree. The X-chromosomal genes *AR* and in cases with uninformative *AR* also *PCSK1N* (located on Xp11.23) (Bertelsen et al., 2011) were amplified in both digested and non-digested DNA samples according to standard PCR conditions (Bertelsen et al., 2011). Fragment length analysis was performed on an ABI 3730 Genetic Analyzer (Thermo Fisher Scientific, Waltham, Massachusetts, USA).

To calculate the degree of XCI, fragment sizes and peak areas from each sample were analyzed with GeneMapper™ (Thermo Fisher Scientific, Waltham, Massachusetts, USA) including the digested and non-digested approaches. In an informative case, the software supplies two major peaks with different lengths for each approach: the short one labeled XC1 and the long one XC2. The area under these curves was used to determine the degree of XCI (X-inactivation ratio, XCR) as described earlier (Echevarria et al., 2016). XCR was defined "skewed," if the distribution was ≥75:25%; all other cases were categorized as "random" (Dobrovolny et al., 2005; Echevarria et al., 2016). When more than one sample of tissue was collected (i.e., a biological replicate), we determined the XCR for each tissue and calculated the average of the XCI. This was the case for 21 mouth epithelial and 28 blood XCR. When the XCI pattern was skewed, we determined the active X-chromosome. For this, we compared the allele length of the PCR products with the ones in the samples of related men or related women where the mutation status was known and classified patients as "mutated X is active" and "mutated X is inactive."

2.7 | Statistical analysis

Continuous data are given either as absolute numbers or median and range. Categorical data are presented as percentages. We used SPSS 27 for statistical analysis (IBM, Ehningen, Germany). Since data were not normally distributed, we used the Mann–Whitney-U test for group comparisons and the Chi^2-test. Correlation analysis was performed by the Spearman test (ρ). p-values $< .05$ were assumed statistically significant.

3 | RESULTS

3.1 | Patient cohort and biomaterial

We recruited 104 women and 50 related men. We excluded 9/104 (9%) women since six had intronic variants or 5′UTR substitutions and three were not informative for the genes *AR* and *PCSK1N*. Hence, further analysis was performed using biomaterial of 95 women and 50 men; 45/95 (47%) women were related. The median age of the female cohort was 53 years (range 18–77) and of the male cohort 42 years (range 18–74). From the female cohort, we collected 94/95 (99%) mouth epithelial cells, 94/95 (99%) blood, and 30/95 (32%) skin fibroblast samples. From the male cohort, we only collected 50/50 (100%) mouth epithelial cells (Figure 1).

3.2 | Classification of sequence variants

We found 48 different sequence variants in the female cohort of 95 women (Table 1). 5/95 (5%) women had more than one variant, whereby all variants were on the same

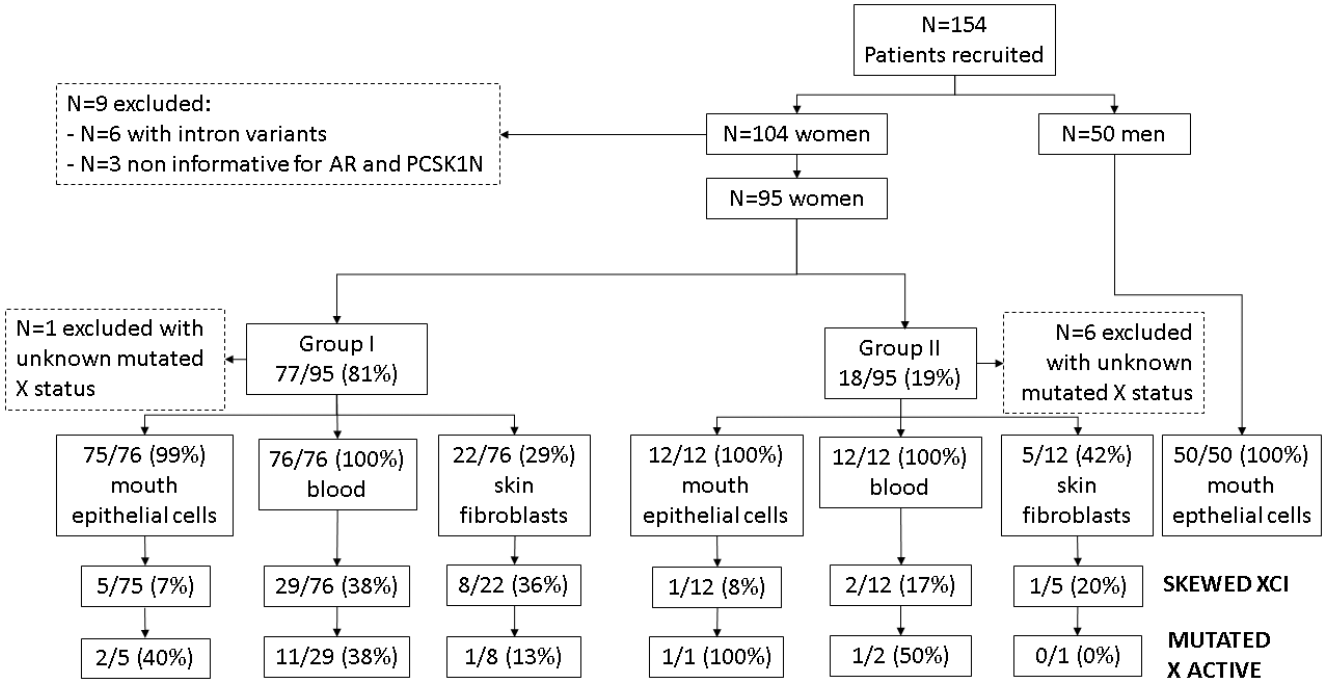

FIGURE 1 Synopsis of the collected biomaterial and XCI patterns. Group I: women carrying potentially pathogenic variants in the alpha-galactosidase A gene; Group II: women carrying variants in the alpha-galactosidase A gene currently classified apathogenic. In seven patients the status of the mutated X-chromosome could not be determined since these women did not have relatives. AR, androgen receptor; PCSK1N, proprotein convertase subtilisin/kexin Typ 1 inhibitor; XCI, X-chromosomal inactivation.

allele. For categorization, we used the one with the putatively higher clinical impact (Supplementary Table S1). Table 2 summarizes details on the distribution of the mutations found. Most women had mutations categorized as classic (43/95, 45%) or class 5 (38/95, 40%). Of the 70/95 (74%) women carrying missense variants, the majority had "other" mutations (44/70, 62%). 18/95 (19%) women carried one of the sequence variants D313Y (9/95, 9%), A143T (8/95, 8%), and W399S (1/95, 1%), which are currently assumed apathogenic (Lenders et al., 2016; Lukas et al., 2016; Oder et al., 2016). Clinical data of the main patient cohort ("Group I", $n = 77$) was assessed separately from the data of these women ("Group II", $n = 18$).

3.3 | XCI patterns and clinical phenotype

Table 3 summarizes the clinical phenotype of the patient cohort. 90/95 (95%) of women were informative (i.e., we obtained a result from the XCI analysis of the respective gene) for *AR and* 5/95 (5%) for *PCSK1N*. A total of 94 mouth epithelial cell and blood samples and 30 skin fibroblast samples were available for XCI pattern analysis. XCI patterns differed between the three biomaterials in individual cases (Table 4) and were skewed in 6/87 (7%) mouth epithelial cells (Group I: 5/75, 7%; Group II: 1/12, 8%), 31/88 (35%) blood samples (Group I: 29/76, 38%; Group II: 2/12, 17%), and 9/27 (33%) in skin fibroblasts (Group I: 8/22, 36%; Group II: 1/5, 20%) (Figure 1). The reciprocal number of women showed random XCI patterns each.

3.4 | Activation status of the mutated X-chromosome in the blood is not associated with disease burden

We continued our analysis by stratifying patient groups for the results of blood data since blood reflected the highest number of women with skewed XCI (31/88, 35%). In these 31 women, the mutated X-chromosome was active in 12/31 (39%) cases (Group I: 11/29, 38%; Group II: 1/2, 50%) (Figures 1–3).

In Group I, GAL showed a trend to lower activity and lyso-Gb3 to higher levels in women with the mutated X-chromosome active compared to those with the mutated X-chromosome inactive, however, differences did not reach statistical significance (Figures 2 and 4a,b). While cardiomyopathy and nephropathy showed a tendency to be more frequent in women with the mutated X-chromosome active (cardiomyopathy: 7/11, 64%; nephropathy: 6/11, 55%) versus those with the mutated X-chromosome inactive (cardiomyopathy: 10/18, 56%; nephropathy: 8/18, 44%), the difference did not reach statistical significance

TABLE 1 Genotypes of the female cohort

		Classification based on			
	Sequence variants	**Clinical phenotype[a]**	**Pathogenicity class[b]**	**localization[c]**	**Frequency**
Missense	c.137A > G//p.H46R	classic	4	buried	1
	c.155G > C//p.C52S	classic	3+	other	1
	c.188G > A//p.C63Y	classic	4	other	2
	c.334C > T//p.R112C	classic	5	buried	1
	c.350 T > G//p.I117S	classic	4	buried	1
	c.386 T > C//p.L129P	classic	4	buried	1
	c.404C > T//p.A135V	classic	4	buried	5
	c.408 T > A//p.D136E	classic	3+	buried	2
	c.416A > G//p.N139S	late onset	2	other	1
	c.427G > A//p.A143T	benign	2	other	8
	c.471G > C//p.Q157H	VUS	3	buried	1
	c.484 T > G//p.W162G	classic	3+	buried	1
	c.486G > T//W162C	classic	3+	buried	1
	c.515G > A//p.C172Y	classic	3+	active site	3
	c.559A > G//p.M187V	classic	3+	buried	1
	c.612G > T//p.W204C	classic	3+	buried	1
	c.644A > G//p.N215S	late onset	5	other	16
	c.806 T > G//p. V269G	classic	4	buried	1
	c.860G > C//p.W287S	VUS	3+	buried	1
	c.902G > A//p.R301Q	late onset	5	other	3
	c.937G > T//p. D313Y	benign	2	other	9
	c.973G > A//p.G325S	late onset	3+	other	1
	c.1025G > T//p.R342L	classic	3	buried	3
	c.1184G > C//p.G395A	likely late onset	3	other	2
	c.1196G > C//p.W399S	benign	2	other	1
	c.1250 T > C//p.L417P	VUS	3	buried	2
Nonsense	c.648 T > A//p.Y216*	VUS	5	NA	2
	c.934C > T//p.Q312*	classic	5	NA	2
	c.1196G > A//p.W399*	classic	5	NA	1
Frameshift	c.290del//p.A97Vfs*24	VUS	5	NA	1
	c.363del//p.N122Ifs*8	classic	5	NA	1
	c.568del//p.A190Pfs*2	classic	5	NA	1
	c.757del//p.I253Lfs*16	VUS	5	NA	3
	c.718_719del//p.K240Efs*9	classic	5	NA	1
	c.927del//p.L310Sfs*7	VUS	5	NA	1
	c.994dup//p.R332Kfs*7	classic	5	NA	3
	c.1223del//p.N408Ifs*10	classic	5	NA	2
Deletion/ delins	c.35_58del//p.C12_A20delinsS	classic	3	NA	1
	c.354_368del//p.Q119_Y123del	classic	3	NA	1
	c.963_964delinsCA//p. Q321_D322delinsHN	classic	3	NA	1
	c.1072_1074del//p.E358del	classic	4	NA	1
Essential splice site	c.369 + 1G > A	classic	5	NA	1
	c.547 + 1G > A	classic	3+	NA	1
	c.802-3_802-2del	classic	3+	NA	1

(Continues)

TABLE 1 (Continued)

	Sequence variants	Classification based on			Frequency
		Clinical phenotype[a]	Pathogenicity class[b]	localization[c]	
Intronic	c.370-10C > T	VUS	3	NA	2
	c.370-81_370-77del	VUS	1	NA	1
	c.640-16A > G	VUS	1	NA	1
	c.1000-22C > T	VUS	1	NA	4

Abbreviations: NA, not applicable; VUS, variant of unknown significance.

[a]According to http://www.dbfgp.org.

[b]1 = benign, 2 = likely benign, 3 = VUS, 3+ = VUS with probable pathogenicity, 4 = likely pathogenic, 5 = pathogenic (Kolokotronis et al., 2020; Richards et al., 2015).

[c]active site mutation = variant in the active site of the alpha-galactosidase A, buried mutation = variant close to active site, other mutation = variant outside the active site (Rickert et al., 2020).

TABLE 2 Distribution of the sequence variants applying three classification systems

Clinical phenotype	
Classic	43/95 (45%)
(Likely) late onset	23/95 (24%)
Benign	18/95 (19%)
VUS	11/95 (12%)
Pathogenicity class	
1	0/95 (0%)
2	10/95 (11%)
3	12/95 (13%)
3+	14/95 (15%)
4	13/95 (14%)
5	38/95 (40%)
Localization	
Active site	3/70 (4%)
Buried	23/70 (32%)
Other	44/70 (62%)

Abbreviations: VUS, variant of unknown significance.

TABLE 3 Distribution of clinical symptoms relative to the number of women in the study cohort where the respective information was available

	Group I[a]	Group II[b]
Cornea verticillata	29/47 (62%)	1/5 (20%)
Cardiomyopathy	43/76 (55%)	1/12 (8%)
Pain	38/74 (51%)	5/11 (45%)
Ear-nose-throat symptoms (including tinnitus, dizziness, sudden deafness)	39/76 (51%)	6/12 (50%)
Nephropathy	32/76 (42%)	1/12 (8%)
An−/hypohidrosis	17/75 (23%)	3/12 (25%)
Gastrointestinal symptoms	17/76 (22%)	5/12 (42%)
SFN	15/76 (20%)	3/12 (25%)
Angiokeratoma	13/68 (19%)	1/12 (8%)
Cerebral stroke	7/76 (9%)	4/12 (33%)
TIA	4/76 (5%)	0/12 (0%)

Abbreviations: SFN, small fiber neuropathy; TIA, transient ischemic attack.

[a]Group I contains $n = 77$ women with pathogenic sequence variants. Those with unknown mutated X status ($n = 1$) are excluded here.

[b]Group II contains $n = 18$ women with apathogenic sequence variants: D313Y, A143T, and W399S. Those with unknown mutated X status ($n = 6$) are excluded here.

(Figure 4c–f). Also, individual analysis of cardiac septum thickness and heart weight, as well as GFR and albuminuria did not reveal intergroup differences (Figure 4c–f). Similarly, the number of patients with the central nervous system (stroke, TIA) and peripheral nervous system symptoms (FD-associated pain, SFN, hypo−/anhidrosis, elevated thermal thresholds) was not different between groups (Figures 2 and 4g,h). This was also true for the overall clinical scores showing a tendency toward more severe phenotypes in the group of women with the mutated X-chromosome active, where, e.g., no case was found without organ involvement, but 4/11 (36%) women with severe disease burden compared to 7/18 (39%) each in the group of women with the mutated X-chromosome inactive (Figure 2). Patient subgroups did not differ in the number of women who received FD-specific treatment (Figure 2). In Group II, the mutated X-chromosome was active only in the blood sample of one patient, hence, no statistical analysis was possible (Figure 3).

3.5 | Skewed XCI with the mutated X-chromosome active is rare in mouth epithelial cells and skin fibroblasts

In mouth epithelial cells (Group I: 5/75, 7%; Group II: 1/12, 8%) and skin fibroblasts (Group I: 8/22,

TABLE 4 Individual XCI patterns

ID	Genotype	Mouth epithelial cells	Blood	Skin fibroblasts	Number of individually skewed tissues	Clinical score (0 = no symptoms; 1 = mild; 2 = moderate; 3 ≥ severe)
Group I						
FD 1005	p.N139S	52:48	68:32	–	0/2	2
FD 1019	p.R332Kfs*7	54:46	**82:18 Xi**	–	1/2	3
FD 1025	p.G325S	72:28	59:41	–	0/2	2
FD 1026	p.A135V	29:71	29:71	–	0/2	1
FD 1027	p.A135V	**21:79 Xa**	33:67	**0:100 Xa**	2/3	0
FD 1032	p.R342L	33:67	**23:77 Xi**	34:66	1/3	3
FD 1035	p.R342L	31:69	**24:76 Xi**	–	1/2	3
FD 1036	p.W204C	48:52	70:30	–	0/2	2
FD 1040	p.N122Ifs*8	60:40	54:46	48:52	0/3	3
FD 1044	p.L129P	56:44	52:48	–	0/2	4
FD 1045	p.C52S	32:68	57:43	–	0/2	1
FD 1048	p. V269G	–	**95:5 Xi**	56:44	1/2	3
FD 1049	p.W399*	30:70	**20:80 Xi**	–	1/2	1
FD 1056	p.Q157H	59:41	60:40	–	0/2	3
FD 1064	p.N215S	45:55	**80:20 Xi**	–	1/2	0
FD 1074	p.I253Lfs*16	39:61	54:46	30:70	0/3	2
FD 1077	p.W287S	36:64	59:41	**91:9 Xi**	1/3	1
FD 1086	p.W162G	47:53	58:42	–	0/2	4
FD 1087	p.A135V	50:50	32:68	–	0/2	1
FD 1088	p.A135V	31:69	30:70	–	0/2	1
FD 1090	p.R332Kfs*7	48:52	57:43	–	0/2	1
FD 1092	p.Q321_ D322delinsHN	43:57	28:72	–	0/2	3
FD 1099	p.K240Efs*9	68:32	**81:19 Xi**	**91:9 Xi**	2/3	3
FD 1104	p.N215S	74:26	**75:25 Xi**	**94:6 Xi**	2/3	2
FD 1110	p.Y216*	41:59	52:48	–	0/2	1
FD 1111	p.Y216*	43:57	52:48	–	0/2	1
FD 1113	p.N215S	47:53	35:65	–	0/2	0
FD 1125	p.R301Q	56:44	**21:79 Xi**	–	1/2	0
FD 1127	p.A135V	34:66	**2:98 Xa**	–	1/2	3
FD 1129	p.D136E	**24:76 Xi**	46:54	–	1/2	1
FD 1131	p.L417P	52:48	**24:76 Xi**	–	1/2	3
FD 1132	p.L417P	49:51	41:59	–	0/2	3
FD 1136	c.369 + 1G > A	37:63	45:55	–	0/2	0
FD 1139	p.E358del	39:61	70:30	30:70	0/3	3
FD 1141	p.N215S	29:71	27:73	–	0/2	2
FD 1146	p.N215S	44:56	60:40	–	0/2	0
FD 1152	p.A190Pfs*2	41:59	36:64	26:74	0/3	2
FD 1156	p.R112C	53:47	43:57	–	0/2	3
FD 1159	p.M187V	42:58	29:71	–	0/2	1
FD 1160	p.N215S	59:41	**92:8 Xi**	65:35	1/3	1

(Continues)

TABLE 4 (Continued)

ID	Genotype	Mouth epithelial cells	Blood	Skin fibroblasts	Number of individually skewed tissues	Clinical score (0 = no symptoms; 1 = mild; 2 = moderate; 3 ≥ severe)
FD 1162	p.Q312*	50:50	46:54	–	0/2	1
FD 1163	p.Q312*	47:53	46:54	–	0/2	2
FD 1164	p.C172Y	52:48	49:51	–	0/2	0
FD 1166	p.A97Vfs*24	38:62	53:47	–	0/2	1
FD 1168	p.N215S	46:54	44:56	–	0/2	0
FD 1174	p.G395A	60:40	34:66	**2:98 Xi**	1/3	1
FD 1175	p.N215S	30:70	**22:78 Xi**	–	1/2	1
FD 1176	p.Q119_Y123del	39:61	59:41	26:74	0/3	2
FD 1182	p.D136E	**83:17 Xi**	**98:2 Xi**	–	2/2	2
FD 1185	p.N215S	**75:25 Xi**	**87:13 Xi**	**96:4 Xi**	3/3	0
FD 1189	p.R301Q	68:32	**87:13 Xa**	–	1/2	1
FD 1190	p.R342L	35:65	**17:83 Xa**	57:43	1/3	2
FD 1193	c.547 + 1G > A	55:45	**76:24 Xa**	–	1/2	4
FD 1196	p.N408Ifs*10	68:32	**83:17 Xa**	–	1/2	4
FD 1198	p.C63Y	50:50	35:65	–	0/2	2
FD 1200	p.N408Ifs*10	39:61	**15:85 Xa**	–	1/2	2
FD 1202	p.N215S	58:42	**10:90 Xa**	–	1/2	1
FD 1203	p.R301Q	39:61	50:50	–	0/2	0
FD 1204	p.G395A	31:69	**4:96 Xi**	**13:87 Xi**	2/3	0
FD 1207	p.N215S	54:46	**85:15 Xa**	–	1/2	3
FD 1209	p.C172Y	44:56	39:61	–	0/2	2
FD 1211	p.C172Y	37:63	28:72	–	0/2	1
FD 1212	p.N215S	37:63	**6:94 Xi**	–	1/2	3
FD 1213	p.I117S	**23:77 Xa**	**16:84 Xa**	53:47	2/2	2
FD 1214	p.L310Sfs*7	52:48	45:55	40:60	0/3	0
FD 1216	p.N215S	36:64	**5:95 Xa**	**79:21 Xi**	2/3	1
FD 1217	p.H46R	42:58	34:66	32:68	0/3	2
FD 1218	p.W162C	51:49	50:50	–	0/2	0
FD 1219	p.R332Kfs*7	66:34	63:37	–	0/2	2
FD 1220	p.N215S	34:66	30:70	–	0/2	1
FD 1222	p.I253Lfs*16	40:60	40:60	74:26	0/3	2
FD 1223	p.C63Y	36:64	**20:80 Xi**	–	1/2	0
FD 1225	p.N215S	47:53	**76:24 Xa**	–	1/2	1
FD 1228	p.N215S	44:56	63:37	–	0/2	0
FD 1230	p.I253Lfs*16	53:47	**77:23 Xi**	–	1/2	2
FD 1234	p.C12_A20delinsS	37:63	46:54	57:43	0/3	2
Group II						
FD 1003	p.A143T	54:46	45:55	–	0/2	1
FD 1053	p.D313Y	42:58	38:62	–	0/2	0
FD 1085	p.A143T	44:56	38:62	38:62	0/3	2[a]
FD 1098	p.D313Y	49:51	66:34	73:27	0/3	0
FD 1114	p.A143T	57:43	49:51	–	0/2	1
FD 1135	p.A143T	54:46	73:27	–	0/2	1

TABLE 4 (Continued)

ID	Genotype	Mouth epithelial cells	Blood	Skin fibroblasts	Number of individually skewed tissues	Clinical score (0 = no symptoms; 1 = mild; 2 = moderate; 3 ≥ severe)
FD 1147	p.D313Y	54:46	51:49	–	0/2	1
FD 1183	p.D313Y	57:43	32:68	49:51	0/3	1
FD 1188	p.A143T	48:52	**76:24 Xi**	45:55	1/3	0
FD 1194	p.D313Y	47:53	44:56	–	0/2	1
FD 1201	p.A143T	62:38	47:53	–	0/2	1
FD 1232	p.D313Y	**25:75 Xa**	**18:82 Xa**	**95:5 Xi**	3/3	2[b]

Note: Bold XCI shows skewing.

Abbreviations: FD, Fabry disease; ID, identification number; Xa, mutated X-chromosome active; Xi, mutated X-chromosome inactive; "–", no sample available.

[a]Patient with chronic widespread pain and cerebral infarction.

[b]Patient with nephropathy due to arterial hypertension and chronic pain syndrome. Kidney biopsy without Gb3 depositions.

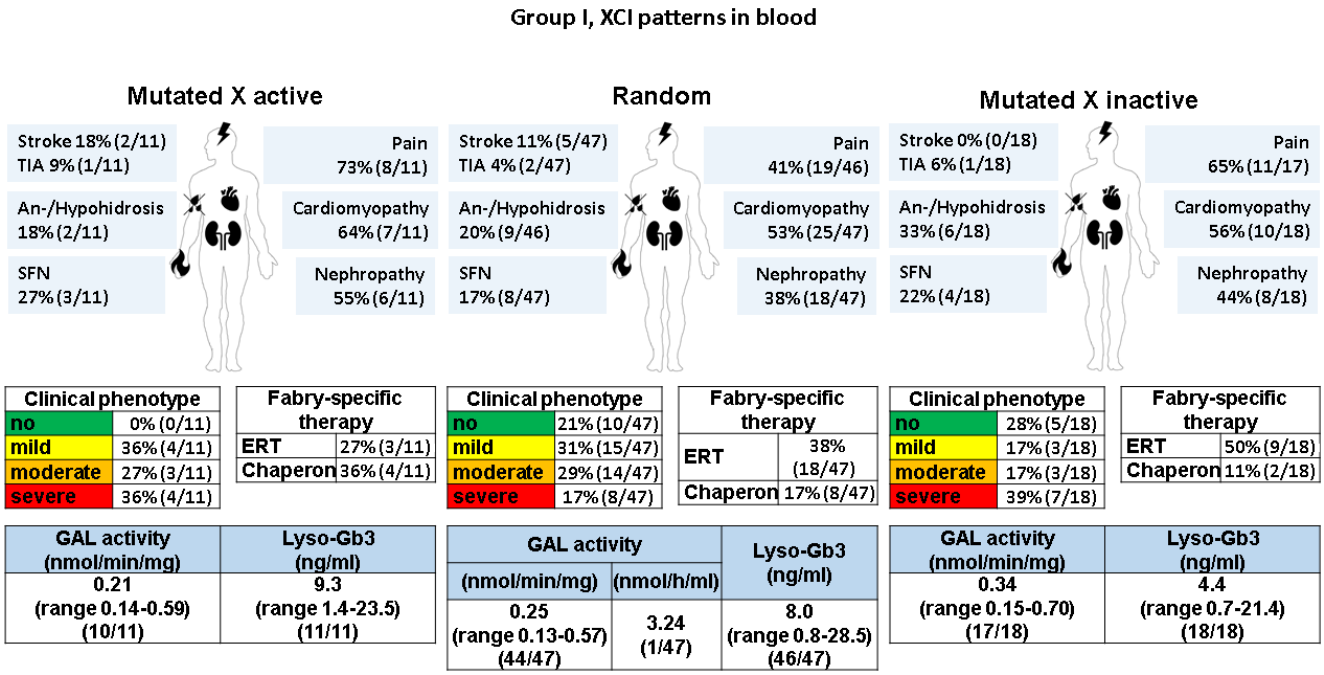

FIGURE 2 XCI patterns and clinical phenotype based on stratification via blood samples in group I. Group I: women carrying potentially pathogenic variants in the alpha-galactosidase A gene. ERT, enzyme replacement therapy; GAL, alpha-galactosidase A; SFN, small fiber neuropathy; TIA, transient ischemic attack; XCI, X-chromosomal inactivation.

36%; Group II: 1/5, 20%), the number of women with skewed XCI was lower compared to blood samples. Also, the mutated X-chromosome was active only in a few women (mouth epithelial cells: Group I: 2/5, 40%; Group II: 1/1, 100%; skin fibroblasts: Group I: 1/8, 13%; Group II: 0/1, 0%) (Figure 1; Supplementary Figures S1–S4). Hence, correlation analysis with the clinical phenotype was not possible. Table 4 gives a synopsis of the clinical phenotype related to patients' genotype and XCI status.

3.6 | XCI patterns remain stable for at least 2 years

To answer the question, if female XCI patterns change over time, we assessed ≥2 biosamples from one tissue of 49 patients collected at two time points with a median latency of 1 year (range 0.2–3.0). Overall, we collected 42 mouth epithelial cell samples obtained from 21/95 (22%) women and 60 blood samples obtained from 28/95 (29%) women. After a median latency of 0.6 years (range

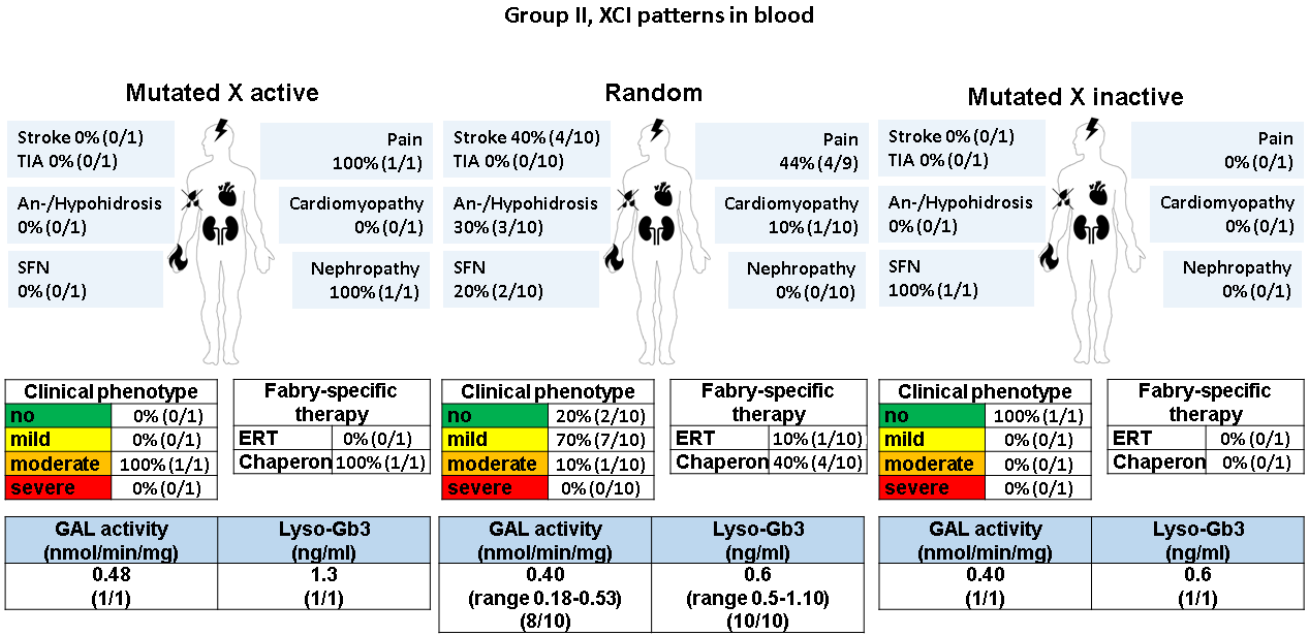

FIGURE 3 XCI patterns and clinical phenotype based on stratification via blood in group II. Group II: women carrying variants in the alpha-galactosidase A gene currently classified apathogenic. ERT, enzyme replacement therapy; GAL, alpha-galactosidase A; SFN, small fiber neuropathy; TIA, transient ischemic attack; XCI, X-chromosomal inactivation.

0.2–1.3) between the first and second mouth epithelial sample collection, the median difference of the XCR was 6% (range 0–19; $\rho = 0.86$, $p < .001$) (Figure 5). After a median of 1.6 years (range 0.2–3.0) upon first blood sample collection, XCR also showed a median shift of 6% (range 0–25%; $\rho = 0.91$, $p < .001$) (Figure 5). Analysis of 65 technical replicates from 29/95 (31%) patients (i.e., a second or third analysis of the XCI pattern from the same sample) revealed robust results with a median shift in XCR of 5% (range 0–48; $\rho = 0.87$, $p < .001$) (Figure 6). Hence, the used method shows high reliability considering the technical replicates. This enables the individual and inter-individual comparison of the XCR. Also, taking this fact into account, the XCR in biological replicates remains stable over time without relevant changes in the XCI.

4 | DISCUSSION

We have investigated XCI patterns related to the activation status of the mutated X-chromosome in a clinically well-characterized, single-center cohort of women carrying genetic variants in the *GLA* gene and using DNA from three different tissues and additionally determining the activation status of the mutated allele. While venous blood was most informative, no correlation was found between the XCI patterns and patients' clinical phenotype. Also, GAL activity and lyso-Gb3 levels did not correlate with the female XCI pattern.

Although of X-chromosomal inheritance, women with FD may reach every level of disease severity, and the reason for this is unknown. XCI is a mechanism that may influence disease penetrance, which was already shown for Duchenne muscular dystrophy and hemophilia A and B (Garagiola et al., 2021; Mercier et al., 2013). In previous studies, XCI patterns were also investigated in women with FD giving contradictory results. While some studies found data suggesting a role of XCI in symptom severity of women with FD (Dobrovolny et al., 2005; Echevarria et al., 2016; Hossain et al., 2019), others did not (Elstein et al., 2012; Juchniewicz et al., 2018; Rossanti et al., 2021; Viggiano & Politano, 2021).

In a previous study, XCR determined in blood and skin fibroblasts correlated with symptom severity scores in FD

FIGURE 4 Inter-group comparison stratified for XCI patterns in group I and based on blood. Scatter plots illustrate the distribution of alpha-galactosidase A activity (a), lyso-Gb3 levels (b), cardiac septum thickness (c), heart weight (d), glomerular filtration rate (e), albumin/creatinine ratio (f), cold detection thresholds (g), and warm detection thresholds (h) between women with skewed XCI and the mutated X-chromosome active or inactive and a random XCI pattern. CDT, cold detection threshold; GAL, alpha-galactosidase A; Gb3, globotriaosylceramide; GFR, glomerular filtration rate; WDT, warm detection threshold.

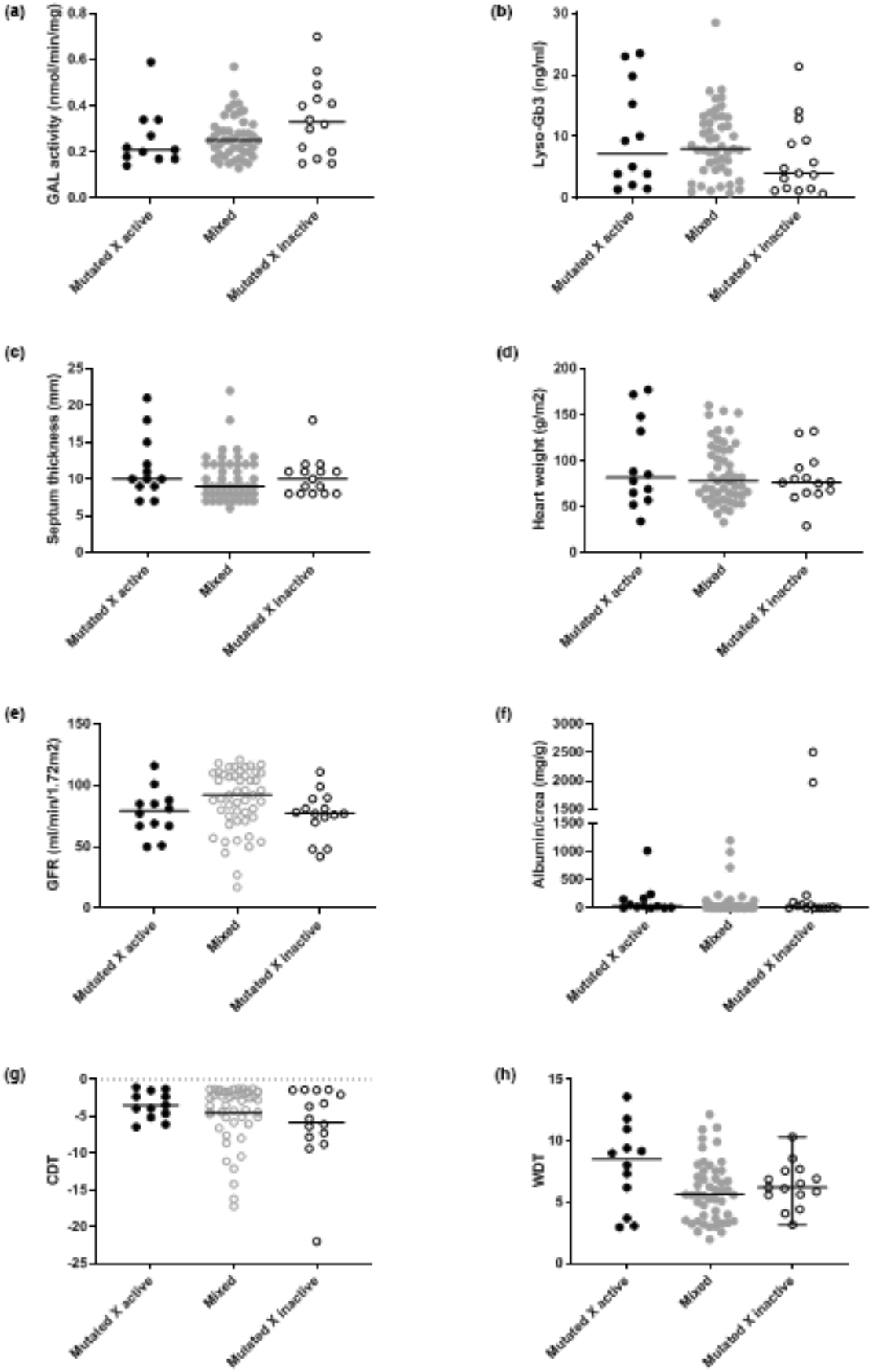
(a)
GAL activity (nmol/min/mg)
0.0
0.2
0.4
0.6
0.8
Mutated X active
Mixed
Mutated X inactive
(b)
Lyso-Gb3 (ng/ml)
0
10
20
30
Mutated X active
Mixed
Mutated X inactive
(c)
Septum thickness (mm)
0
5
10
15
20
25
Mutated X active
Mixed
Mutated X inactive
(d)
Heart weight (g/m2)
0
50
100
150
200
Mutated X active
Mixed
Mutated X inactive
(e)
GFR (ml/min/1.72m2)
0
50
100
150
Mutated X active
Mixed
Mutated X inactive
(f)
Albumin/crea (mg/g)
0
500
1000
1500
1500
2000
2500
3000
Mutated X active
Mixed
Mutated X inactive
(g)
CDT
0
-5
-10
-15
-20
-25
Mutated X active
Mixed
Mutated X inactive
(h)
WDT
0
5
10
15
Mutated X active
Mixed
Mutated X inactive

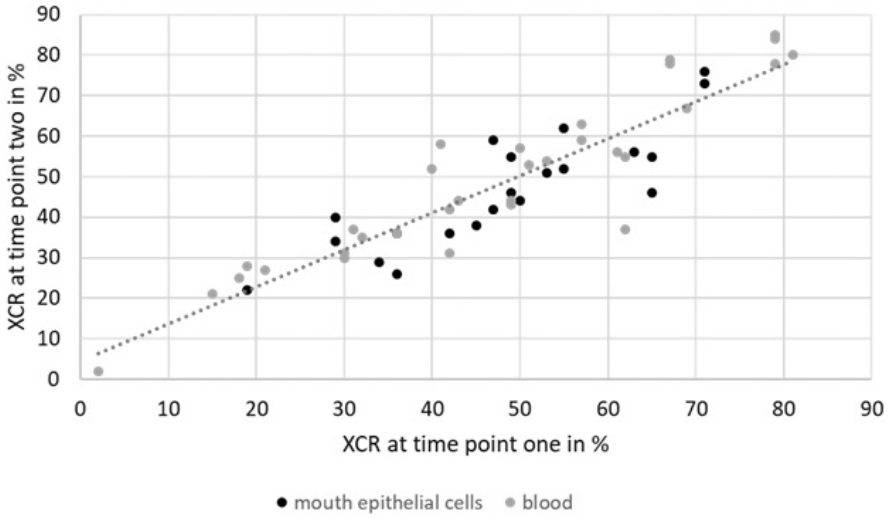

FIGURE 5 XCR in biological replicates of mouth epithelial cells and blood samples. The graph illustrates the correlation of the XCR at two time points with data points obtained using mouth epithelial cells ($\rho = 0.86$, $p < .001$) and blood samples ($\rho = 0.91$, $p < .001$). XCR, X-inactivation ratio.

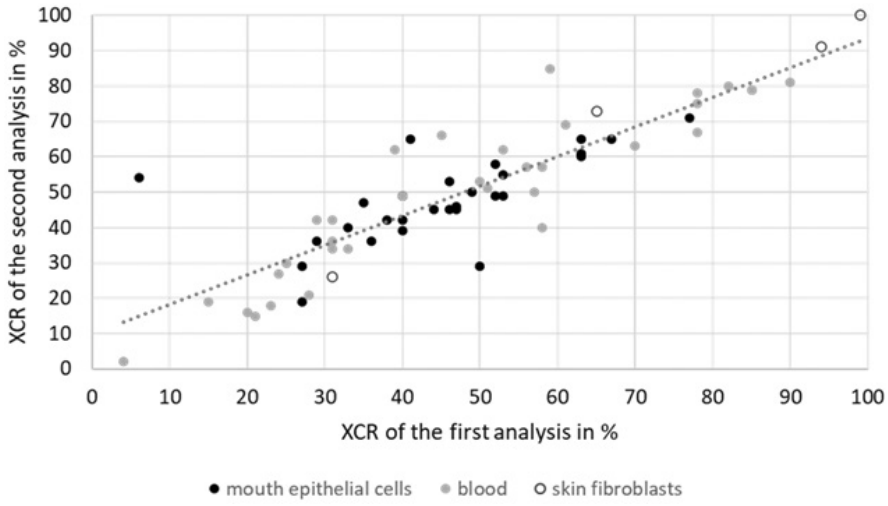

FIGURE 6 XCR in technical replicates. The graph illustrates the correlation between the first and second analyses of the same biomaterial ($\rho = 0.87$, $p < .001$). XCR, X-inactivation ratio.

(Dobrovolny et al., 2005). Similar results were reported in a study investigating XCI patterns in mouth epithelial cells, blood, urine, and skin fibroblasts (Echevarria et al., 2016). However, data cannot be compared directly, since Echevarria et al. (2016) defined a "skewed XCI pattern" when more than one tissue showed skewed XCR. We did not find a correlation between the individual XCI patterns of FD women and symptom severity in line with several other studies (Elstein et al., 2012; Juchniewicz et al., 2018; Rossanti et al., 2021), albeit the number of investigated FD women was small in these studies ($n = 12$ and $n = 9$) and a skewed XCI pattern was found only in one of these patients (Juchniewicz et al., 2018; Rossanti et al., 2021). Further, without determining whether the mutated or the healthy allele is active (Elstein et al., 2012), data interpretation is not possible. In our study, blood was the biomaterial most frequently revealing skewed XCI. Skin fibroblasts gave similar results, but biological relevance remains obscure due to the low number of skin punch biopsies available. Mouth epithelial cells were obtained from almost the entire study cohort, however, XCI patterns were mostly not skewed. This diversity of XCI patterns found in different cell types is a known phenomenon (Zito et al., 2019), the reason for which is elusive.

Our data show the relevance of genetic subclassification in clinical practice: women carrying classic, class 3+ and higher, and the active site or buried mutations (Arends et al., 2017; Rickert et al., 2020) also had a more severe clinical phenotype (Figure 2, Tables 1 and 4). However, XCI patterns did not show additive effects in our cohort.

One crucial question is if XCR individually remains stable over time. The biological replicates we investigated showed XCR stability over 2 years, which was the longest period possible in our study (Figure 5). Assessment of XCI patterns in healthy women revealed that the rate of skewing rises from 16% to 38% between the age of ≤32 to ≥60 years (Busque et al., 1996). In another study, a skewing ratio of approximately 40% was described in healthy aging women when assessed in blood samples (Busque et al., 2009). Also, high skewing rates were more frequent

in blood samples obtained from women ≥60 years (Sharp et al., 2000). Hence, prospective and long-term studies are needed to answer the question of at which age and after which interval XCI pattern analysis would be most informative.

Our data further show that the method used to determine XCI patterns results in similar XCR within a median difference of 5% when repeatedly analyzing the same biosample (Figure 6). This enables the comparison of samples collected from one patient between the same and other tissues and the comparison with the XCR among all patients. Our results are in line with those of a previous study which determined repeatability of 3% for the assay used (Busque et al., 2009).

Another question is if XCI patterns differ between biomaterials. We found that the XCI pattern was not different between mouth epithelial cells, blood, and skin fibroblast samples considering the classification in skewed and random XCI in approximately 60–70% cases (data not shown), which is in line with data from previous studies (Dobrovolny et al., 2005; Echevarria et al., 2016; Rossanti et al., 2021). Also, the incidence of random XCI patterns found in blood and skin fibroblast samples reported in other studies is similar to ours (70% versus 65–67%) (Dobrovolny et al., 2005; Echevarria et al., 2016; Elstein et al., 2012). When comparing XCI patterns in all three tissues, we found a deviation to skewing mainly in blood samples. The median age of the subpopulation of women with skewed XCI between the tissues (36/95, 38%) was 57 years (range 26–74), which fits data of a previous study investigating XCI patterns of healthy women: here, a higher frequency of skewed XCI was found at >60 years and also larger inter-tissue deviations of XCI patterns were described with aging (Sharp et al., 2000).

Further, it is crucial to determine the X-chromosome that carries the mutated allele to conclude the usefulness of XCI patterns in clinical practice. This was also achieved in some previous studies through comparison with relatives (Dobrovolny et al., 2005; Echevarria et al., 2016; Juchniewicz et al., 2018). We and others used biomaterial that is easily available but not primarily affected by FD such as heart, kidneys, and nervous tissue. Hence, it remains elusive if and to which extent results obtained in mouth epithelial cells, blood, and fibroblasts can reflect disease severity. Another crucial issue to be considered is that tissues from different embryonic layers can have different X-inactivation patterns (Viggiano et al., 2013). Further, the phenomenon that some genes may "escape" X-chromosomal inactivation needs attention, since this might also contribute to the diversity in clinical phenotypes of women with FD (Carrel & Willard, 2005).

One limitation of our study is that we could not apply validated clinical scoring systems such as the Mainz Severity Score Index (MSSI) due to missing data, since the majority of patients were recruited during follow-up visits that included a focused investigation program. Another limitation of our study is that we used a scoring system that does not reflect mono- versus multiorgan involvement. Also, our patient cohort includes variants of FD with organ-specific clinical phenotypes such as N215S, which may have influenced the clinical composite score used. However, we have also investigated organ-specific parameters and believe that the impact on the overall results is minor if any. Approximately half of the study population was on FD-specific treatment, which we could not stop for our study for ethical reasons and which may have contributed to modify the clinical phenotype.

We show that blood as an easily available biomaterial most frequently reflects skewed XCI patterns in women carrying genetic variants in *GLA*, while these patterns do not correlate with disease severity. We conclude that further studies investigating larger patient cohorts including longitudinal investigation, and using biomaterial obtained from organs primarily affected by FD are needed to understand the pathophysiological role XCI patterns may play in the disease development of women with FD.

AUTHOR CONTRIBUTIONS

Nurcan Üçeyler and Simone Rost created the study concept and research design. Laura Wagenhäuser collected data and performed analysis. Vanessa Rickert collected data. Laura Wagenhäuser, Simone Rost, Nurcan Üçeyler performed analysis and data interpretation. Nurcan Üçeyler, Claudia Sommer, Christoph Wanner, Peter Nordbeck performed patient examination. Nurcan Üçeyler, Laura Wagenhäuser, Simone Rost wrote the manuscript. All authors reviewed the manuscript and approved the final version of the paper.

ACKNOWLEDGMENTS

Expert technical help by Daniela Urlaub and Barbara Broll (Department of Neurology, University of Würzburg, Germany), Birgit Halliger-Keller (Institute of Human Genetics, University of Würzburg, Germany), and Irina Schumacher (Würzburg Fabry Center for Interdisciplinary Therapy, FAZIT, University of Würzburg, Germany) is gratefully acknowledged. Open Access funding enabled and organized by Projekt DEAL.

FUNDING INFORMATION

The study was supported by an Investigator-Initiated Research grant (no. IIR-DEU-000798)", provided by Takeda Pharmaceuticals International AG. The sponsor had no knowledge of the data and the manuscript

was exclusively written by the authors. N.Ü. was supported by the German Research Foundation (Deutsche Forschungsgemeinschaft, DFG: UE171-15/1). Further funding was received by the Collaborative Research Center (SFB 1158, DFG).

CONFLICT OF INTEREST

The authors declare the following conflicts of interest: L.W., V.R., and S.R. report no conflicts of interest. C.S. has received honoraria for lectures from Amicus and Takeda. P.N. has received travel grants and honoraria for lectures from Amicus Therapeutics, Chiesi, Idorsia, Greenovation, Sanofi Genzyme, and Takeda Shire, and research funds from Amicus Therapeutics, Idorsia Sanofi Genzyme, and Takeda Shire. CW has received honoraria from Amicus, Chiesi, Idorsia, Sanofi-Genzyme, and Shire-Takeda for advisory board activities and lecturing. N.Ü. has received travel grants and honoraria for lectures from Sanofi Genzyme and Takeda Shire, and research funds from Sanofi Genzyme, Takeda Shire, and Idorsia.

DATA AVAILABILITY STATEMENT

Data are available upon request from the corresponding author. Data are not publicly available due to privacy or ethical restrictions.

ORCID

Peter Nordbeck https://orcid.org/0000-0002-2560-4068
Nurcan Üçeyler https://orcid.org/0000-0001-6973-6428

REFERENCES

Allen, R. C., Zoghbi, H., Moseley, A., Rosenblatt, H. M., & Belmont, J. (1992). Methylation of HpaII and HhaI sites near the polymorphic CAG repeat in the human androgen-receptor gene correlates with X chromosome inactivation. *American Journal of Human Genetics*, *51*, 1229–1239.

Arends, M., Wanner, C., Hughes, D., Mehta, A., Oder, D., Watkinson, O. T., Elliott, P. M., Linthorst, G. E., Wijburg, F. A., Biegstraaten, M., & Hollak, C. E. (2017). Characterization of classical and nonclassical Fabry disease: A multicenter study. *Journal of the American Society of Nephrology*, *28*, 1631–1641.

Bertelsen, B., Tümer, Z., & Ravn, K. (2011). Three new loci for determining X chromosome inactivation patterns. *The Journal of Molecular Diagnostics*, *13*, 537–540.

Busque, L., Mio, R., Mattioli, J., Brais, E., Blais, N., Lalonde, Y., Maragh, M., & Gilliland, D. G. (1996). Nonrandom X-inactivation patterns in normal females: Lyonization ratios vary with age. *Blood*, *88*, 59–65.

Busque, L., Paquette, Y., Provost, S., Roy, D. C., Levine, R. L., Mollica, L., & Gary Gilliland, D. (2009). Skewing of X-inactivation ratios in blood cells of aging women is confirmed by independent methodologies. *Blood*, *113*, 3472–3474.

Carrel, L., & Willard, H. F. (2005). X-inactivation profile reveals extensive variability in X-linked gene expression in females. *Nature*, *434*, 400–404.

Delano, W. L. (2015). *The PyMOL molecular graphics system*. Schrödinger, Inc.

Devigili, G., Tugnoli, V., Penza, P., Camozzi, F., Lombardi, R., Melli, G., Broglio, L., Granieri, E., & Lauria, G. (2008). The diagnostic criteria for small fibre neuropathy: From symptoms to neuropathology. *Brain*, *131*, 1912–1925.

Dobrovolny, R., Dvorakova, L., Ledvinova, J., Magage, S., Bultas, J., Lubanda, J. C., Elleder, M., Karetova, D., Pavlikova, M., & Hrebicek, M. (2005). Relationship between X-inactivation and clinical involvement in Fabry heterozygotes. Eleven novel mutations in the alpha-galactosidase a gene in the Czech and Slovak population. *Journal of Molecular Medicine (Berlin, Germany)*, *83*, 647–654.

Echevarria, L., Benistan, K., Toussaint, A., Dubourg, O., Hagege, A. A., Eladari, D., Jabbour, F., Beldjord, C., de Mazancourt, P., & Germain, D. P. (2016). X-chromosome inactivation in female patients with Fabry disease. *Clinical Genetics*, *89*, 44–54.

Elstein, D., Schachamorov, E., Beeri, R., & Altarescu, G. (2012). X-inactivation in Fabry disease. *Gene*, *505*, 266–268.

Garagiola, I., Mortarino, M., Siboni, S. M., Boscarino, M., Mancuso, M. E., Biganzoli, M., Santagostino, E., & Peyvandi, F. (2021). X chromosome inactivation: A modifier of factor VIII and IX plasma levels and bleeding phenotype in Haemophilia carriers. *European Journal of Human Genetics*, *29*, 241–249.

Garman, S. C., & Garboczi, D. N. (2004). The molecular defect leading to Fabry disease: Structure of human alpha-galactosidase. *Journal of Molecular Biology*, *337*, 319–335.

Germain, D. P. (2010). Fabry disease. *Orphanet Journal of Rare Diseases*, *5*, 30.

Hossain, M. A., Wu, C., Yanagisawa, H., Miyajima, T., Akiyama, K., & Eto, Y. (2019). Future clinical and biochemical predictions of Fabry disease in females by methylation studies of the GLA gene. *Molecular Genetics and Metabolism Reports*, *20*, 100497.

Juchniewicz, P., Kloska, A., Tylki-Szymańska, A., Jakóbkiewicz-Banecka, J., Węgrzyn, G., Moskot, M., Gabig-Cimińska, M., & Piotrowska, E. (2018). Female Fabry disease patients and X-chromosome inactivation. *Gene*, *641*, 259–264.

Karl, F., Wußmann, M., Kreß, L., Malzacher, T., Fey, P., Groeber-Becker, F., & Üçeyler, N. (2019). Patient-derived in vitro skin models for investigation of small fiber pathology. *Annals of Clinical Translational Neurology*, *6*, 1797–1806.

Kolokotronis, K., Pluta, N., Klopocki, E., Kunstmann, E., Messroghli, D., Maack, C., Tejman-Yarden, S., Arad, M., Rost, S., & Gerull, B. (2020). New insights on genetic diagnostics in cardiomyopathy and arrhythmia patients gained by stepwise exome data analysis. *Journal of Clinical Medicine*, *9*.

Lenders, M., Weidemann, F., Kurschat, C., Canaan-Kühl, S., Duning, T., Stypmann, J., Schmitz, B., Reiermann, S., Krämer, J., Blaschke, D., Wanner, C., Brand, S. M., & Brand, E. (2016). Alpha-galactosidase a p.A143T, a non-Fabry disease-causing variant. *Orphanet Journal of Rare Diseases*, *11*, 54.

Lukas, J., Scalia, S., Eichler, S., Pockrandt, A. M., Dehn, N., Cozma, C., Giese, A. K., & Rolfs, A. (2016). Functional and clinical consequences of novel α-galactosidase a mutations in Fabry disease. *Human Mutation*, *37*, 43–51.

Magg, B., Riegler, C., Wiedmann, S., Heuschmann, P., Sommer, C., & Üçeyler, N. (2015). Self-administered version of the Fabry-associated pain questionnaire for adult patients. *Orphanet Journal of Rare Diseases*, *10*, 113.

Mercier, S., Toutain, A., Toussaint, A., Raynaud, M., de Barace, C., Marcorelles, P., Pasquier, L., Blayau, M., Espil, C., Parent, P., Journel, H., Lazaro, L., Andoni Urtizberea, J., Moerman, A., Faivre, L., Eymard, B., Maincent, K., Gherardi, R., Chaigne, D., … Desguerre, I. (2013). Genetic and clinical specificity of 26 symptomatic carriers for dystrophinopathies at pediatric age. *European Journal of Human Genetics*, *21*, 855–863.

Oder, D., Üçeyler, N., Liu, D., Hu, K., Petritsch, B., Sommer, C., Ertl, G., Wanner, C., & Nordbeck, P. (2016). Organ manifestations and long-term outcome of Fabry disease in patients with the GLA haplotype D313Y. *BMJ Open*, *6*, e010422.

Richards, S., Aziz, N., Bale, S., Bick, D., das, S., Gastier-Foster, J., Grody, W. W., Hegde, M., Lyon, E., Spector, E., Voelkerding, K., Rehm, H. L., & ACMG Laboratory Quality Assurance Committee. (2015). Standards and guidelines for the interpretation of sequence variants: A joint consensus recommendation of the American College of Medical Genetics and Genomics and the Association for Molecular Pathology. *Genetics in Medicine*, *17*, 405–424.

Rickert, V., Wagenhäuser, L., Nordbeck, P., Wanner, C., Sommer, C., Rost, S., & Üçeyler, N. (2020). Stratification of Fabry mutations in clinical practice: A closer look at alpha-galactosidase A-3D structure. *Journal of Internal Medicine*, *288*, 593–604.

Rossanti, R., Nozu, K., Fukunaga, A., Nagano, C., Horinouchi, T., Yamamura, T., Sakakibara, N., Minamikawa, S., Ishiko, S., Aoto, Y., Okada, E., Ninchoji, T., Kato, N., Maruyama, S., Kono, K., Nishi, S., Iijima, K., & Fujii, H. (2021). X-chromosome inactivation patterns in females with Fabry disease examined by both ultra-deep RNA sequencing and methylation-dependent assay. *Clinical and Experimental Nephrology*, *25*, 1224–1230.

Sharp, A., Robinson, D., & Jacobs, P. (2000). Age- and tissue-specific variation of X chromosome inactivation ratios in normal women. *Human Genetics*, *107*, 343–349.

Üçeyler, N., Kafke, W., Riediger, N., He, L., Necula, G., Toyka, K. V., & Sommer, C. (2010). Elevated proinflammatory cytokine expression in affected skin in small fiber neuropathy. *Neurology*, *74*, 1806–1813.

Viggiano, E., Picillo, E., Cirillo, A., & Politano, L. (2013). Comparison of X-chromosome inactivation in Duchenne muscle/myocardium-manifesting carriers, non-manifesting carriers and related daughters. *Clinical Genetics*, *84*, 265–270.

Viggiano, E., & Politano, L. (2021). X chromosome inactivation in carriers of Fabry disease: Review and meta-analysis. *International Journal of Molecular Sciences*, *22*.

Wilcox, W. R., Oliveira, J. P., Hopkin, R. J., Ortiz, A., Banikazemi, M., Feldt-Rasmussen, U., Sims, K., Waldek, S., Pastores, G. M., Lee, P., Eng, C. M., Marodi, L., Stanford, K. E., Breunig, F., Wanner, C., Warnock, D. G., Lemay, R. M., Germain, D. P., & Fabry Registry. (2008). Females with Fabry disease frequently have major organ involvement: Lessons from the Fabry registry. *Molecular Genetics and Metabolism*, *93*, 112–128.

Zito, A., Davies, M. N., Tsai, P. C., Roberts, S., Andres-Ejarque, R., Nardone, S., Bell, J. T., Wong, C. C. Y., & Small, K. S. (2019). Heritability of skewed X-inactivation in female twins is tissue-specific and associated with age. *Nature Communications*, *10*, 5339.

SUPPORTING INFORMATION

Additional supporting information can be found online in the Supporting Information section at the end of this article.

How to cite this article: Wagenhäuser, L., Rickert, V., Sommer, C., Wanner, C., Nordbeck, P., Rost, S., & Üçeyler, N. (2022). X-chromosomal inactivation patterns in women with Fabry disease. *Molecular Genetics & Genomic Medicine*, *10*, e2029. https://doi.org/10.1002/mgg3.2029